

Characterization of Propagation Models at 5G Network and Effects of SAR on Human Brain

Nawal Al-Aamri, Zia Nadir, Mohammed Bait-Suwailam, and Hassan Al-Lawati

Abstract—Nowadays, the world is turning into technology, fast internet and high signal quality. To ensure high signal quality, the network planners have to predict the pathloss and signal strength of the transmitted signal at specific distances in the design stage. The aim of this research is to provide a generalized pathloss model to suit the urban area in Muscat Governorate in the Sultanate of Oman. The research covers 5G network pathloss in the Muttrah Business District (MBD) area. It includes Close In (CI) model and Alpha Beta Gamma (ABG) model with 3.45GHz. The results of 5G models were compared with real experimental data in MBD by calculating Root Mean Square Error RMSE. Other cells at MBD area were used for reverification. To validate the modified pathloss models of 5G, they were applied at different cells in Alkhoud area. Furthermore, this paper also deals the effect of Specific Absorption Rate (SAR) on the human brain for ensuring safety due to close proximity to cell towers. The SAR values were calculated indirectly from the electric field strength of different antennas. Calculated results were compared with the international standards defined limits on the human brain.

Keywords—pathloss; prediction; 5G; RMSE; CI model; ABG model; SAR

I. INTRODUCTION

THE 5G is nowadays a communication standard. It came to overcome the former networks' challenges and shortcomings. 5G network is providing high speed internet and higher bandwidth with data rate of more than 10Gbps. Its latency is around 1ms or less. It is lower than 4G latency by ten times [1]. 4G is focusing only on data transfer rate, the 5G is concentrating on Enhanced Mobile Broadband (eMBB), Ultra-Reliable and Low Latency Communication (URLLC) and Massive Machine Type Communication (mMTC). It means 5G technology is ready to increase the number of users and connected devices. It can contain 1million connections in 1km². The 5G technology changes the meaning of communications. It outperforms other technologies. Based on 5G, new technology revolutions are built. It moves from communication between people to things communication. Internet of things is the main application supported by 5G. In this generation, connected devices will be via an intelligent communication network. In 5G, the virtual network becomes part of any new network. The 5G reliability motivates all life aspects to employ the technology. The new situation in COVID-19 pandemic changes the lifestyle. Health care, education, businesses and other sectors are using extensive online networks. The pandemic highlights the technology's ability to cover the demands by a

critical secure network. The new technology in the cellular network creates new opportunities for people and organizations. It facilitates all difficulties. Smart health care (eHealth), e-learning, smart transportation, big data analysis, virtual network, smart cities, block chain, clouds, IoT, AI and other terms become familiar to all society categories [2]. 5G subscribers are increasing rapidly as a result of these applications.

With the high demand for the network, we pay our attention in this research on how the operators will provide an efficient network with high quality. It requests the operator to plan the network properly to reach this goal. The well planned signal propagation needs pathloss prediction tools. The pathloss prediction models are introduced in this paper for 5G network. The attenuation which may happen on signals can be predicted in the design stage. Thus, the parameters can be decided early to reduce losses. There are many propagation models studying the pathloss and predicting the signal strength at a specific distance for 5G cellular network in urban terrain. None of these models are specified for the Sultanate of Oman. This research objective is to develop Pathloss prediction models suitable for proposed urban areas for 5G cellular network to be used by RF planners. The research depends on Omantel collected data from MBD area. The research also aims to verify the developed models by applying them in different cells in MBD and Alkhoud areas and calculating RMSE as error indicator using (1). The RMSE calculation depends on finding the error between experimental pathloss and predicted pathloss. The RMSE should be limited [3].

$$RMSE = \sqrt{\frac{\sum(P_m - P_r)^2}{(N-1)}} \quad (1)$$

Where,

P_m : Experimental Pathloss [dB]

P_r : Predicted Pathloss [dB]

N : Number of experimental values

Moreover, this research targets to calculate the SAR value and conformity of the results with international standards. As there are rapid spread of new technologies and high demand of smart applications, the service providers have to provide enough network coverage. These lead them to provide more base stations. This part of the research will brief how the new technologies are safe for different mechanisms especially for the human brain.

This work was supported by ECE dept. at SQU and Omantel team.

Authors are with ECE dept. at college of Engineering at SQU, Muscat, Sultanate of Oman. (email: s69729@student.squ.edu.om; nadir@squ.edu.om; msuwailem@squ.edu.om; hlawati@squ.edu.om).



© The Author(s). This is an open-access article distributed under the terms of the Creative Commons Attribution License (CC BY 4.0, <https://creativecommons.org/licenses/by/4.0/>), which permits use, distribution, and reproduction in any medium, provided that the Article is properly cited.

II. STUDIES AND RESEARCH

A. 5G Studies and Research

Referring to a study done by researchers from Bangladesh in 2020 [4], the researchers used ABG and CI models to choose the best modulation systems for 5G using 28GHz with different filters. The resulted BER gave good results with CI model in most calculations comparing to ABG model. Considering the new technologies in the research which was done in 2017 in Kuwait [5] for 5G technologies with 28GHz, the researchers found that the Ericsson model is the best for the urban environment. The researchers in [6] did a study in 2017 in Malaysia using 15GHz in 5G network. They employed microcell propagation model and Okumura-Hata model. However, they recommended implementing the CI, Floating Intercept (FI) and ABG models as they were more efficient as per their findings.

Similar to the above researches, many other researches were done around the world specifying their results for specific locations indoor or outdoor. These researches focused on identifying an appropriate model for a specific location with a particular frequency or modifying existing models to suit their environment similar to this research objective. Practically no model can suit all environments perfectly.

In general, none of these studies were done in the Sultanate of Oman covering 5G networks. The research [3, 7, 8] were done in the Sultanate of Oman for 2G,3G and 4G networks using the Okumura Hata model, the Extended Sakagami model and the Cost231 model. Unlike this current research which covers 5G network pathloss prediction models.

B. SAR Studies and Research

There were several previous studies, done by different researchers studying SAR effect on different human tissues. The research [9] was done in China. The researchers used simulations to study SAR resulted from 5G network. The research presented the SAR values on the human brain resulted from antennas operated at 2.6GHz and 3.5GHz. The SAR values were 0.217 W/kg and 0.285 W/kg respectively. They concluded the SAR value which reached to the brain was 0.25 from total SAR.

A different methodology was followed in [10]. The researchers used ESM 120 meter and ESM 140 meter to measure the SAR resulted from phones which were connected to 900MHz network. The maximum resulting SAR was 0.5mW/kg. Another study was done in India in 2020 [11]. It focused on the effect of SAR on the children's head and how they differ from an adult. Their research resulted in higher SAR on children' head than adults resulted from mobile phone radiations due to low thickness of children tissues.

The researchers from Sri Lanka did a research in 2019 to calculate SAR on the human brain and eye which resulted from antenna operated at different frequencies through simulations [12]. They summarized their work by proposing that the SAR depended on the electric properties of tissue and not on the shape or size. Many other research was done internationally in different aspects. They included SAR which resulted from phones, base stations or other radiation sources. The researchers followed different ways to find SAR values. Simulation softwares, measurement tools and using SAR equations support to find SAR.

III. PATHLOSS MODELS

A. Close-in (CI) Free Space Reference Distance Model

Close-in model is based on the relationship between pathloss and distance. Equation (2) is used to calculate CI model [13]. Where (3) is free space pathloss $PLFS(d_o)$ at reference distance $d_o = 1m$. Where d_o is close-in reference distance and λ is wavelength.

Equation (4) is the new expression of $PLFS(d_o)$ after substituting $d_o=1m$ in (3). Where frequency (f) in Hz and speed of light (c) is in meter are replacing λ . Pathloss Exponent PLE (n) differs with different environments. PLE demonstrates the relation between signal strength and distance and how the signal decreases when distance grows. Table I lists PLE values [14, 15]. The table I shows that with availability of obstacles between transmitter and receiver, the PLE value increases. For example, in free space $n=2$, means less pathloss and high received power. The PLE increases with availability of obstructions.

In this research n is chosen to be between 2.7-3.5 for urban area. The pathloss will be calculated with different n values within this range.

$$PL[d] = PLFS(d_o) + 10n \log_{10}\left(\frac{d}{d_o}\right) \quad (2)$$

$$PLFS[d_o] = 20 \log_{10}\left(\frac{4\pi d_o}{\lambda}\right) \quad (3)$$

$$PLFS[d_o] = 20 \log_{10}\left(\frac{4\pi f}{c}\right) \text{ when } d_o = 1m \quad (4)$$

TABLE I
PATHLOSS EXPONENT VALUES FOR DIFFERENT ENVIRONMENTS [14]

Environment	PLE (n)
Free space	2
Urban area cellular radio	2.7-3.5
Shadowed urban cellular radio	3-5
In building line of sight	1.6-1.8
Obstructed in building	4-6
Obstructed in factories	2-3

B. ABG Model

Alfa, Beta, Gama model considers distance and frequency. In contrast with CI model which is affected by one exponent (n), the ABG model is affected by α, β, γ . Where α and γ are distance and frequency coefficients. β is an optimized offset value for PL in dB [4]. α, β, γ values will be determined from Table II for different environments. These values are the ITU recommendation for above roof top propagation in different environments taking into account frequency range and distance range. Equation (5) is ABG pathloss expression $PL^{ABG}(f, d)$ [4]. Where d is distance between MS and BS in meters and f is the frequency in GHz.

For pathloss calculation, α, β, γ are chosen to suit NLoS with frequency 2.2-66.5GHz from Table II.

$$PLFS^{ABG}[f, d] = 10\alpha \log_{10}(d) + \beta + 10\gamma \log_{10}(f_c) \quad (5)$$

TABLE II
Pathloss Coefficients [16]

Frequency range (GHz)	Distance range (m)	Type of environment	LoS/ NLoS	α	β	γ
2.2-73	55-1200	Urban high-rise, Urban low-rise/ Suburban	LoS	2.29	28.6	1.96
2.2-66.5	260-1200	Urban high-rise	NLoS	4.39	-6.27	2.30

IV. 5G PATHLOSS EXPERIMENTAL RESULTS

5G network was tested initially in MBD concentrating on Cell-325. Its results were used to generalize the models. The BS height was 30m, while the used MS height was 1.5m. The network was tested at 3.45GHz frequency. The drive test was done to collect real pathloss. After 5G pathloss models were employed to predict signal pathloss, the following outcomes were achieved. CI model was examined with different Pathloss Exponent (PLE) values. PLE was selected from 2.7-3.5 for the urban area environment. The selected exponents from this range were: 2.7, 3, 3.2 and 3.5.

The α , β , γ values of the ABG model were selected from Table II to suit NLoS urban area equal to 4.39, -6.27, 2.30 respectively. The predicted pathlosses of Cell-325 with the CI model and the ABG model, are shown in Fig.1 in addition to experimental pathloss values. Calculating the pathloss using the original CI model with PLE=2.7 and ABG model gave less difference from experimental data as compared to CI model with PLE=3,3.2 and 3.5. Both predicted path losses were greater than the experimental values by more than 30dB in some distances. As they were designed originally for different environments considering more affected factors in the worst situation than this research environment.

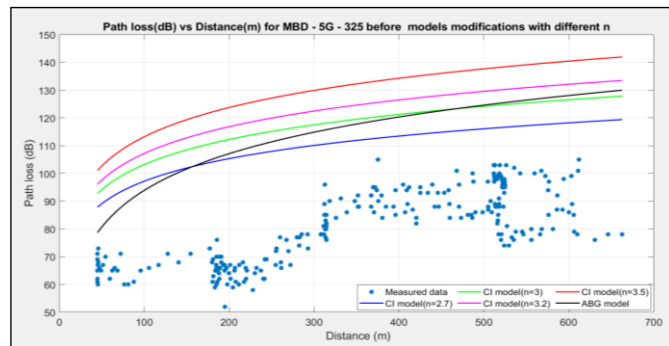


Fig.1. Pathloss for MBD-5G-cell325 Using CI and ABG models

The error between predicted pathloss and experimental pathloss were calculated through RMSE as in Table III. CI model with PLE=2.7 followed by ABG model gave lower RMSE matching the pathloss prediction. In the CI model, as PLE values increased the predicted pathloss increased resulted in high RMSE. In order to get a suitable model for Muscat area, the original models should be modified. By utilizing RMSE in the original models' (6) to (10) were generated to reduce the gap between predicted pathloss and experimental pathloss. The RMSEs were subtracted from the original equations. The RMSE comprises of all known and unknown factors in each model.

TABLE III
RMSE for MBD_5G_Cell 325

Pathloss Model	MBD_5G_Cell 325	
	RMSE (dB)	PLE
CI model	31.07	2.7
	38.20	3
	43.02	3.2
	50.31	3.5
ABG model	35.68	-

Modified CI model with PLE=2.7:

$$PL[d] = PLFS(d_o) + 2.7 * 10\log_{10}\left(\frac{d}{d_o}\right) - 31.07 \quad (6)$$

Modified CI model with PLE=3:

$$PL[d] = PLFS(d_o) + 3.0 * 10\log_{10}\left(\frac{d}{d_o}\right) - 38.20 \quad (7)$$

Modified CI model with PLE=3.2:

$$PL[d] = PLFS(d_o) + 3.2 * 10\log_{10}\left(\frac{d}{d_o}\right) - 43.02 \quad (8)$$

Modified CI model with PLE=3.5:

$$PL[d] = PLFS(d_o) + 3.5 * 10\log_{10}\left(\frac{d}{d_o}\right) - 50.31 \quad (9)$$

Modified ABG model:

$$PLFS^{ABG}[f, d] = 10\alpha \log_{10}(d) + \beta + 10\gamma \log_{10}(f_c) - 35.68 \quad (10)$$

This step should help to predict pathloss close to experimental pathloss. To check their effectiveness, the previous test should be repeated. Cell-325 pathloss was predicted again by modified equations. Fig. 2 shows the predicted and the experimental pathloss.

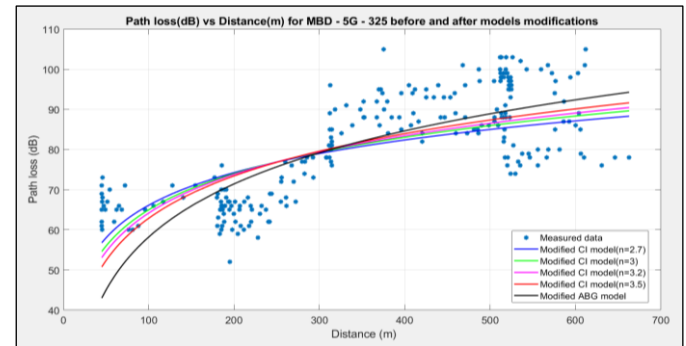


Fig.2. Pathloss for MBD-5G-cell325 Using modified CI and ABG models

The new RMSE values are listed beside the original model RMSE in Table IV. The RMSE values of all models are close to each other. The PLE equal to 3.2 which was used in the CI model gave the lowest RMSE after the models' modification.

TABLE IV
RMSE for MBD_5G_Cell-325

Pathloss Model	MBD_5G_Cell-325		
	RMSE (dB)	RMSE (dB) After model modification	PLE
CI model	31.07	9.24	2.7
	38.20	9.11	3
	43.02	9.08	3.2
	50.31	9.13	3.5
ABG model	35.68	9.87	-

Modified ABG model produced high RMSE. The CI model with PLE=3 was the best in the tested area with RMSE equal to 9.08dB. In general, the modified models predicted very close pathloss to experimental values. The resulted RMSE values of all modified models in the 5G network are acceptable. They indicate model efficiency in MBD area.

To confirm the outputs, the modified ABG model and modified CI model were examined with different cells in MBD and Alkhoud. They worked with the same frequency 3.45GHz. Cell-23 was selected for this purpose in MBD area. Its height was 20m. It was lower than Cell-325 height. Fig. 3 displays the Cell-23 experimental pathloss with predicted pathloss as a function of distance in meter for both models.

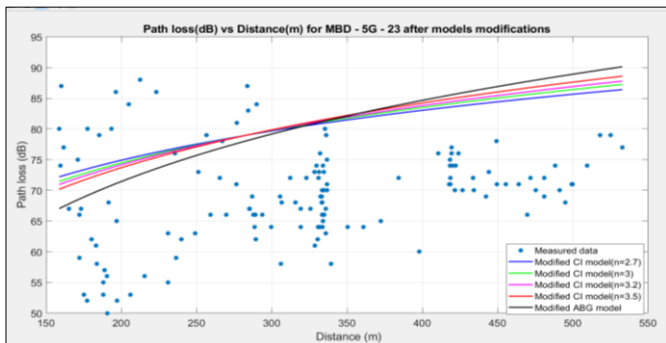


Fig. 3. Pathloss for MBD-5G-cell-23 Using modified CI and ABG models

Table V listed calculated RMSE between experimental and predicted pathloss of cell-23. The recorded RMSE was 13.39dB for the modified ABG model. Whereas, it was 12.58dB for the CI model with PLE=2.7 after model modification. The CI model gave the best result but this time with PLE equal to 2.7. The results of both models are very close to each other. They are accepted while there were some variances between Cell-325 and Cell-23 representing in surrounding buildings and antenna height.

TABLE 5
RMSE for MBD_5G_Cell-23 using modified models

Pathloss Model	MBD_5G_Cell-23	
	RMS \bar{e} (dB)	PLE
	After models modification	
CI model	12.58	2.7
	12.90	3
	13.08	3.2
	13.30	3.5
ABG model	13.39	-

Contrary to Cell-325, the covered area by Cell-23 was quite better with fewer obstructions. Consequently, the drive test measurements provided low values. The experimental pathloss were less than 90dB. This observation raises the RMSE. Additional investigation was done in Alkhoud area. The tested area in Alkhoud was served by three cells in different directions Cell-33, Cell-34 and Cell-35.

The cells were examined by modified models to check the models' performance in the new area by calculating RMSE. Their experimental and predicted pathloss are displayed in Fig.4, 5 and 6. The modified models performed accurately in Alkhoud area. All results show high efficiency in the new locations. The RMSE results from Cell-33, 34 and 35 are listed in Table VI.

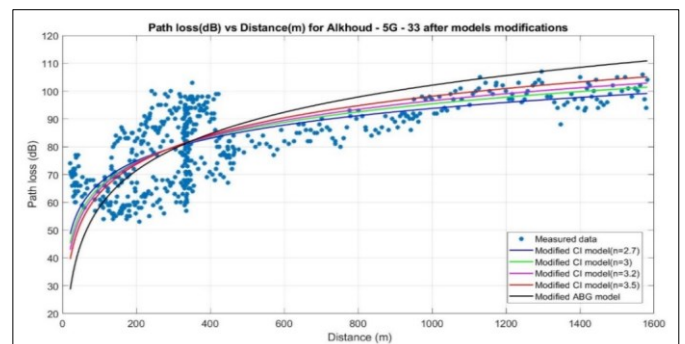


Fig.4. Pathloss for Alkhoud-5G Cell-33 Using modified CI and ABG models

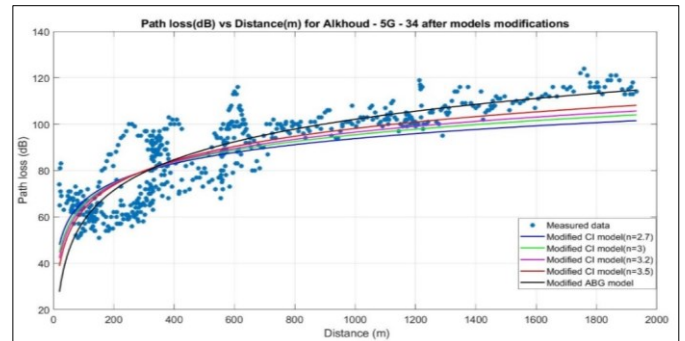


Fig.5. Pathloss for Alkhoud-5G Cell-34 Using modified CI and ABG models

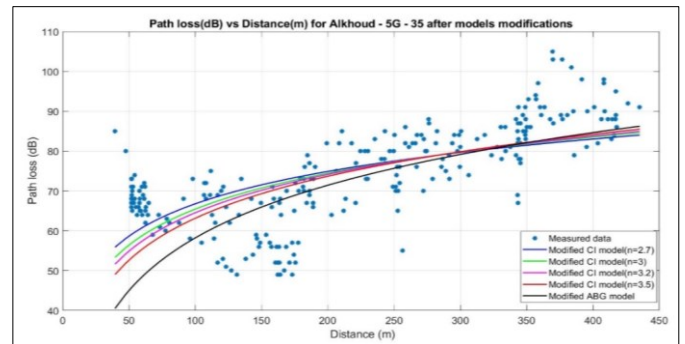


Fig.6. Pathloss for Alkhoud-5G Cell-35 Using modified CI and ABG models

Although there are limited available 5G network, the used models with the selected areas were working fine and giving a good guide for the 5G network planner in the design stage. Generally, both the CI model with PLE 2.7-3.5 and the ABG model were working properly in the urban environment in

Muscat areas. The CI model outperforms the ABG model. The 5G models' performance summary is illustrated in the chart in Fig.7 with reference RMSE line equal to 6dB.

TABLE VI
RMSE for Alkhoud_5G_Cell-33, 34 and 35 using modified models

Pathloss Model	Alkhoud_5G			
	RMSE (dB) using modified models			
	Cell-33	Cell-34	Cell-35	PLE
CI model	10.51	11.72	9.50	2.7
	10.76	11.08	9.59	3
	11.01	10.76	9.70	3.2
	11.49	10.44	9.96	3.5
ABG model	13.46	10.59	11.48	-

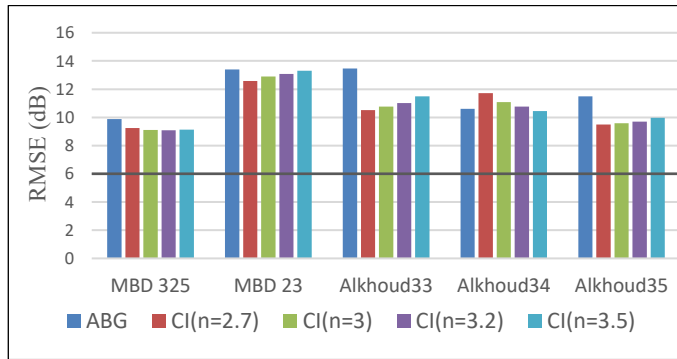


Fig.7. RMSE comparison of 5G network

V. SPECIFIC ABSORPTION RATE SAR

A. SAR Overview

In conjunction with the rapid increase in the availability of communication networks and renewable requirements to keep up to date with technology, the service providers must be careful about the effects of electromagnetic waves on Organisms. Worldwide, there are many standards that control the availability of these, by limiting the allowed radiated power through different electromagnetic elements such as base stations. Including 5G technology in the cellular networks causes public concern due to its high frequency [10]. ICNIRP, IEEE, and FCC are related international organizations providing guidelines, standards and limitations [11]. In the Sultanate of Oman, Telecommunications Regulatory Authority (TRA) regulates everything related to the frequencies and the communications spectrum and usage. This is in addition to The Environment Authority, which also evaluates the negative impacts of different radiation on the environment. These organizations did several studies to provide the standards as per the international permissible limitations.

Specific Absorption Rate (SAR) is one of the most important parameter related to radiations. It is the measurements of absorbed radio frequency RF energy by the human body [11]. It is linked with how much human body tissue absorbs power when faced the EM field [10, 17]. Its unit is (W/kg), which describes the dependency of SAR on absorbed power (W) by human tissue per unit mass of the tissue (kg) [11]. The determined limit of SAR by ICNIRP is 2W/kg. The IEEE specifies SAR equal to 2W/kg for the human head in

unrestricted environments for the frequency range 100 kHz to 6 GHz [18]. Whereas FCC limits for SAR is 1.6 W/kg [11, 18, 19]. Experimental electric field, E (V/m), magnetic field, H (A/m) and power density, P_d (W/m²) were compared with accepted ICNIRP standards [19]. TRA team concentrated on evaluation of frequency, wavelength of RF signal, transmitted power from the antenna and distance from base stations [20].

Different research was done previously on SAR. They studied the effect of SAR on the human body parts. The researchers concentrated on different sources of the EM field. Some of these works simulated the human body parts and how they will be affected by different frequency ranges. In those research, the simulation outcomes were compared with standards. In addition, there are measurement tools measuring SAR in the human body. SAR meter (ESM 120) in Fig.8 is an example of these tools. In some research, it is employed for real time SAR measurements.



Fig.8. SAR meter (ESM 120) [21]

This tool determines the SAR from wireless sources like base stations. Different studies mentioned the effect of SAR on the human brain. They concluded with accepted ranges. SAR level differs between different tissues. In the human head, the scalp and skull are absorbing electromagnetic signals more than the brain. Where the brain is receiving only 0.25 of SAR value. It is about 0.125 times the scalp SAR value [9]. The researchers in [12] concluded that the SAR value was affected mostly by electrical properties of tissues more than its shape and size. It was more in children's head than adults due to its low thickness [11]. In this research, SAR was found by indirect calculations from electric field intensity by (8) [17].

$$SAR = \frac{\sigma E^2}{2\rho} \quad (8)$$

Where σ (sigma) specifies the electrical conductivity of human body parts in S/m [11]. There are different conductivity values for different body tissues. The conductivity values are affected by frequency ranges. As frequency increases, the specific tissue conductivity increases. In SAR calculations of this work, the conductivity is 0.91 S/m and 2.59 S/m were used to calculate SAR for 800MHz and 3.45GHz respectively. ρ (rho) is the mass density (body tissue density). It is measured in kg/m³ [11, 17]. The brain mass density is equal to 1030 kg/m³ [22]. E , The electric field strength is calculated by (9) [23]. Where S is power density in W/m² and Z is the impedance in Ω . The power density and impedance are found with (10) and (11) respectively [24]. The power density S depends on base station transmitted power P_t in watt, antenna gain G and distance in meter [23]. As distance d from transmitter increases, the power density decreases. Consequently, the electric field and SAR decrease. Table VII lists the dielectric properties of the human brain which are implemented in the study for 800MHz and 3.45GHz.

$$E = \sqrt{S * (2 * Z)} \quad (9)$$

$$S = \frac{P_t G}{4 * \pi * d^2} \quad (10)$$

$$Z = Z_o \sqrt{\frac{\mu_r}{\epsilon_r}} \text{ where } \therefore Z_o = 377\Omega \text{ (free space)} \quad (11)$$

TABLE VII
Dielectric properties of the human brain [22, 24, 25]

Frequency	800 MHz	3.45 GHz
Conductivity σ	0.91 S/m	2.59 S/m
Permittivity ϵ_r	53.252	47.379
Mass density ρ	1030 kg/m ³	1030 kg/m ³
Permeability μ_r	1	1

Very clearly, SAR value is impacted by frequency which specifies the conductivity. Also, the distance from a radiation source and antenna parameters (transmitted power and antenna gain) change the SAR values.

B. SAR Experimental Results

In this study, the SAR was calculated on 4G (800MHz) and 5G (3.45GHz) networks in different locations in Muscat Governorate. After applying the equations of SAR calculation in 4G network at MBD, Alkhwair, Algubrah and Alkhoud areas, the resulted SAR are presented in Fig.9, 10, 11and 12. The figures explain the inverse relation between SAR and distance. As distance increases, the SAR decreases.

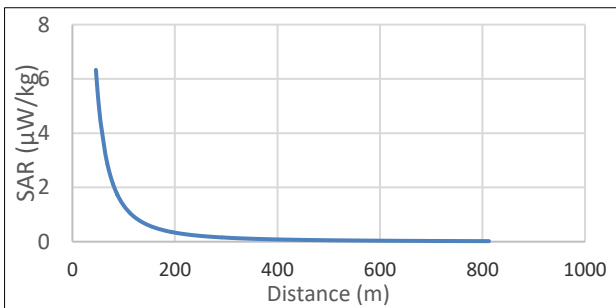


Fig.9. SAR of MBD_4G_Cell-237

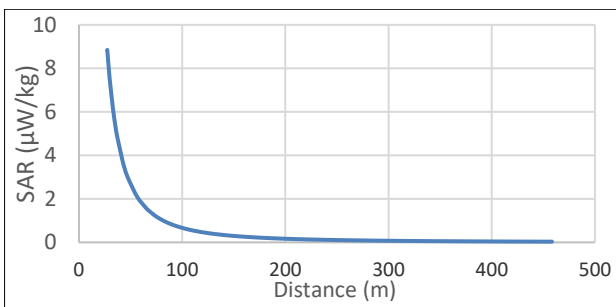


Fig.10. SAR of Alkhwair_4G_Cell-98

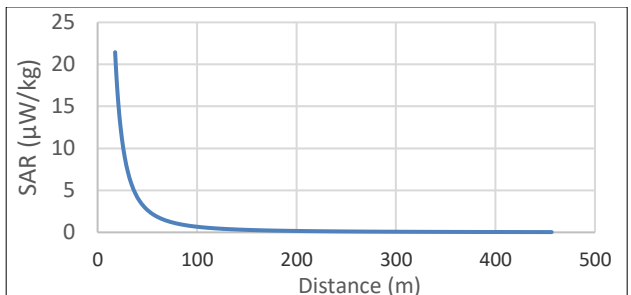


Fig.11. SAR of Algubrah_4G_Cell-287

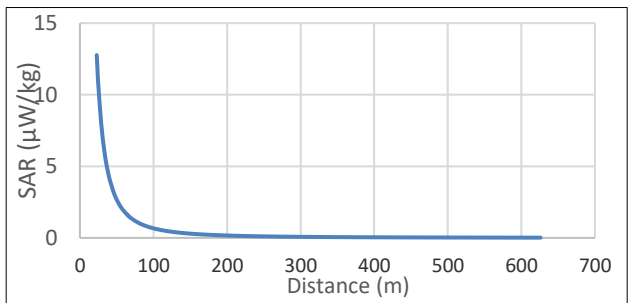


Fig.12. SAR of Alkhoud_4G_Cell-34

As shown in these figures, SAR values of used antennas are very small compared with standards. They didn't exceed 25 µW/kg. The same calculations were repeated with 5G network coverage at 3.45GHz by using suitable dielectric properties.

Fig.13 and 14 illustrate the calculated SAR at 5G network in MBD and Alkhoud area. The 5G network SAR values are higher than the 4G network SAR due to high transmitted power and high frequency. The transmitted powers at the 4G in this research were 18.2dBm in MBD and 15.2dBm in other locations. On the other hand, the transmitted power of the 5G network was 34.9dBm. In 5G, the SAR exceeds 3000 µW/kg. But It didn't reach limitations as per standards. In general, by following the guidelines and standards, we can safely conclude that the organisms under discussion will be safe from the negative impact of EM radiation at these particular frequencies. While the users will benefit from new technologies with high-speed data transfer rate.

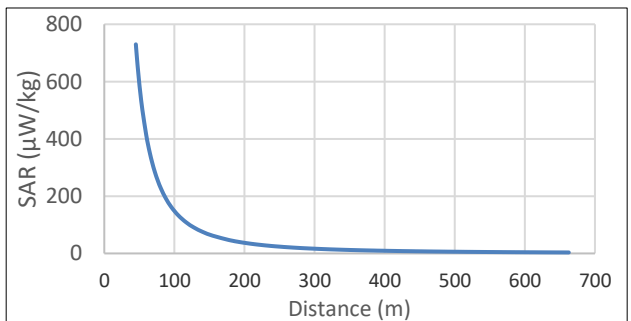


Fig.13. SAR of MBD_5G_Cell-325

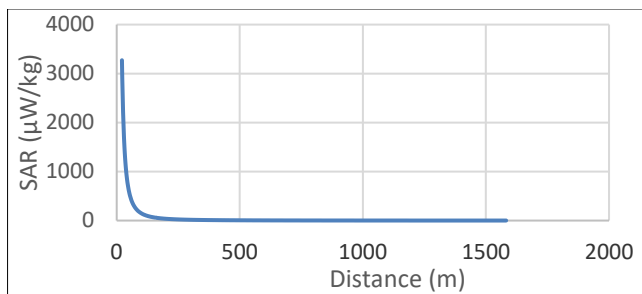


Fig.14 SAR of Alkhoud_5G Cell-33

CONCLUSION

The objective of this research is to identify pathloss models suited for Muscat Governorate in the Sultanate of Oman for 5G networks. The research aim was achieved by employing different pathloss models on the 5G network working at 3.45GHz. The calculations were done via models' equations using MATLAB. This study was the first in the region. From the tested pathloss models and calculated RMSE at 5G network, the modified CI model with PLE range (2.7-3.5) can be used in MBD and Alkhoud for 5G network pathloss prediction. The resulted SAR values from research calculations are lower than the standard limitation.

ACKNOWLEDGEMENTS

The authors would like to express their gratitude to ECE department, Omantel & Huawei team, Eng. Alaa Adein, for their support and drive tests for the successful completion of this study.

REFERENCES

- [1] G. Barb and M. Otesteanu, "4G/5G: A Comparative Study and Overview on What to Expect from 5G," in *2020 43rd International Conference on Telecommunications and Signal Processing (TSP)*, 2020, pp. 37-40. <https://doi.org/10.1109/TSP49548.2020.9163402>
- [2] W. Jiang, B. Han, M. A. Habibi, and H. D. Schotten, "The Road Towards 6G: A Comprehensive Survey," *IEEE Open Journal of the Communications Society*, vol. 2, pp. 334-366, 2021. <https://doi.org/10.1109/OJCOMS.2021.3057679>
- [3] Z. Nadir, H. A. Lawati, and M. A. Rashdi, "Propagation Measurements and Pertinency of Models for Communications Systems in Oman," *American Journal of Science & Engineering (AJSE)*, vol. 1, 2020. <https://dx.doi.org/10.15864/ajse.1403>
- [4] M. H. Mahmud, K. Khaleduzzaman, S. Sarker, and L. C. Paul, "Effect of Path Loss Models on Performance of 5G Compatible MIMO WINDOW-OFDM Systems," in *2020 International Conference on Smart Technologies in Computing, Electrical and Electronics (ICSTCEE)*, 2020, pp. 257-262. <https://doi.org/10.1109/ICSTCEE49637.2020.9277121>
- [5] A. Zreikat and M. Djordjevic, "Performance Analysis of Path loss Prediction Models in Wireless Mobile Networks in Different Propagation Environments," in *Proceedings of the 3rd World Congress on Electrical Engineering and Computer Systems and Science (EECSS'17)*, Rome, Italy, 2017, pp. 103-1-103-11. <https://doi.org/10.11159/vmw17.103>
- [6] F. Qamar, T. Abbas, M. N. Hindia, K. B. Dimyati, K. A. B. Noordin, and I. Ahmed, "Characterization of MIMO propagation channel at 15 GHz for the 5G spectrum," in *2017 IEEE 13th Malaysia International Conference on Communications (MICC)*, 2017, pp. 265-270. <https://doi.org/10.1109/MICC.2017.8311770>
- [7] Z. Nadir and H. A. Lawati, "LTE path-loss prediction models' comparative study for outdoor wireless communications," in *7th Brunei International Conference on Electrical and Computer Engineering (BICEET 2018)*, 2018, pp. 1-4. <https://doi.org/10.1049/cp.2018.1499>
- [8] Z. Nadir and M. Bait-Suwailam, "Pathloss Analysis at 900 MHz for Outdoor Environment," presented at the International Conference on Communications, Signal Processing and Computers, 2014.
- [9] Y. Li and M. Lu, "Study on SAR Distribution of Electromagnetic Exposure of 5G Mobile Antenna in Human Brain," 2020. [https://doi.org/10.6180/jase.202006_23\(2\).0012](https://doi.org/10.6180/jase.202006_23(2).0012)
- [10] J. Michalowska, A. Wac-Włodarczyk, and J. Kozieł, "Monitoring of the Specific Absorption Rate in Terms of Electromagnetic Hazards," *Journal of Ecological Engineering*, vol. 21, pp. 224-230, 2020. <https://doi.org/10.12911/22998993/112878>
- [11] A. D. Sonawane and D. S. Bormane, "A Specific Absorption Rate in Human Head due to Mobile Phone Radiations: Review," in *2020 International Conference on Electronics and Sustainable Communication Systems (ICESC)*, 2020, pp. 703-707. <https://doi.org/10.1109/ICESC48915.2020.9155777>
- [12] A. Karunaratna, C. A. Fernando, and P. Samarasekara, "Effect of shape, size and electrical properties on specific absorption rate (SAR)," *International Journal of Research and Engineering*, vol. 6, 06/01 2019. <https://doi.org/10.21276/ijre.2019.6.3.1>
- [13] Y. Zhang, S. Jyoti, C. R. Anderson, D. J. Love, N. Michelusi, A. Sprintson, et al., "28-GHz Channel Measurements and Modeling for Suburban Environments," in *2018 IEEE International Conference on Communications (ICC)*, 2018, pp. 1-6. <https://doi.org/10.1109/ICC.2018.8422820>
- [14] M. Hamid, "Measurement Based Statistical Model for Path Loss Prediction for Relaying Systems Operating in 1900 MHz Band," Doctorate, Semantic Scholar, 2014.
- [15] T. S. Rappaport, *Wireless Communications Principles and Practice*: Prentice Hall, 2002.
- [16] ITU, "Propagation data and prediction methods for the planning of short-range outdoor radiocommunication systems and radio local area networks in the frequency range 300 MHz to 100 GHz," ed. USA: International Telecommunication Union, 2017, pp. 1-54.
- [17] A. Rashid O. Mumi, R. Alias, J. Abdullah, S. Haimi Dahlan, and J. Ali, "Assessment of Electromagnetic Absorption towards Human Head Using Specific Absorption Rate," 2018, vol. 7, p. 8, 2018-12-01 2018. <https://doi.org/10.11591/eei.v7i4.1357>
- [18] I. C. Society., "IEEE Standard for Safety Levels with Respect to Human Exposure to Electric, Magnetic, and Electromagnetic Fields, 0 Hz to 300 GHz," *IEEE Std C95.1-2019 (Revision of IEEE Std C95.1-2005/Incorporates IEEE Std C95.1-2019/Cor 1-2019)*, pp. 1-312, 2019. <https://doi.org/10.1109/IEEESTD.2019.8859679>
- [19] ICNIRP, "Guidelines for limiting exposure to time-varying electric, magnetic, and electromagnetic fields (up to 300 GHz). International Commission on Non-Ionizing Radiation Protection," *Health Phys.*, vol. 74, pp. 494-522, Apr 1998. <https://doi.org/10.1097/HP.0b013e3181f06c86>
- [20] I. A. Maawali, "Assessment of Electromagnetic Fields Exposure of Telecom Sites," T. R. A. Oman, Ed., ed. 2020.
- [21] MASCHEK, "SAR meter ESM 120," ed. Germany, 2007.
- [22] H. A. Jalal Baayer, "Invention of an Original Tetra-Generations Patch Antenna for the New Generation of Mobile Telephony and the Study of the Thermal Effect of GSM on the Human Head and Hand," presented at the Proceedings of the Third International Conference on Computing and Wireless Communication Systems, ICCWCS 2019, Faculty of Sciences, Ibn Tofail University -Kénitra- Morocco, 2019. <https://doi.org/10.4108/eai.24-4-2019.2284214>
- [23] Giangrandi. (2012, 20 February 2021). *Field generated by a transmitter at a given distance*. Available: <https://www.giangrandi.ch/electronics/anttool/tx-field.shtml>
- [24] T. B. Rashid and H. H. Song, "Analysis of biological effects of cell phone radiation on human body using specific absorption rate and thermoregulatory response," *Microwave and Optical Technology Letters*, vol. 61, pp. 1482-1490, 2019/06/01 2019. <https://doi.org/10.1002/mop.31777>
- [25] N. Carrara. (28 January 2021). *Dielectric Properties of Body Tissues in the frequency range 10 Hz - 100 GHz*. Available: <http://niremf.ifae.cnr.it/tissprop/#over>